2021

RELATING LINEAR AND ROTATIONAL ACCELERATIONS WITH INTERNAL PRESSURES DEVELOPED INSIDE HUMAN HEAD SURROGATE MODELS

Arthur Thomas Koster

RELATING LINEAR AND ROTATIONAL ACCELERATIONS WITH INTERNAL PRESSURES DEVELOPED INSIDE HUMAN HEAD SURROGATE MODELS

By

ARTHUR THOMAS KOSTER

THESIS

Submitted in partial fulfillment of the requirements
for the degree of Master of Science in Aerospace Engineering at
The University of Texas at Arlington
December 2021

Arlington, Texas

Supervising Committee:

Ashfaq Adnan, Supervising Professor
Alan P. Bowling
Kent L. Lawrence

ABSTRACT

Relating Linear and Rotational Accelerations with Internal Pressures Developed Inside Human Head Surrogate Models

Arthur Thomas Koster, M.S.

The University of Texas at Arlington, 2021

Supervising Professor: Ashfaq Adnan

Traumatic Brain Injury (TBI) is a chronic disease process that is difficult to both detect and treat. TBI can result from blast, kinetic, sonic, and electromagnet energy sources. This research focuses on correlating the bulk acceleration of a human-like head model to the localized internal pressure developed in the coup and contrecoup regions due to variable impact loading. Damage resulting in a TBI occurs on a multiscale level from the macroscale down to the damage of each individual neuron. Obtaining a relationship between bulk acceleration and localized internal pressure will allow for further correlation to the damage done on these smaller length scales. Internal pressure information also allows for investigation into whether cavitation occurs inside the head, a potential damage mechanism for TBI. This research effort utilizes an in-house designed and manufactured pendulum test stand for delivery of the controlled impact load. Data acquisition is obtained using a National Instruments Data Acquisition System (DAQ) and a LabVIEW program. Currently, a human-like 3D printed head model is filled with water and varying concentrations of gelatin solution that is used to simulate the fluids contained within the human head. In water tests, impact accelerations of up to 400g can be felt by the head model and this acceleration correlates to roughly a +100 kPa pressure spike in the coup region and a -50 kPa pressure spike in the contrecoup region.

ACKNOWLEDGEMENTS

This work has been funded by the Office of Naval Research (ONR)(Award # N00014-18-1-2082 – and M00014-21-1-2051). Thanks to Dr. Adnan, Dr. Lawrence, and Dr. Bowling.

DEDICATIONS

I dedicate this thesis to my supportive parents, Pam and Brian, and to my brother, Brett, who is always there to cheer me on and show me the way. This would not have been possible without the support of my loving friends Aaron, Ian, Quincy, Daniel, Zach, and Preston or without the support of my lab mates, especially Dr. Fuad Hasan and Dr. Khandakar Abu Hasan Mahmud.

Table of Contents

Table of Figures

Chapter 1
Introduction

Whether on the field of battle or the field of play, about 2 million head injuries occur during a year in the United States resulting in as many as 56,000 deaths. This amounts to about 40% of all trauma injuries in the United States [1]. The tolls of these injuries on individuals and society are significant and warrant a research effort towards increasing the understanding of brain injury and the mechanisms that cause it.

In the past, research with the goal to understand brain injury has taken on many forms. Starting in the 1940s, work was done to relate brain injury to linear and rotational accelerations. Since then, brain injury has also been studied from the perspective of tissue shear and deformation as a damage mechanism [2]. The phenomena that cause brain injury occur on multiple length scales from damaged blood vessels and tissues, skull fractures, to the damage of individual axons. The best understanding of brain injury will be formed when the damage mechanisms at each length scale can be linked. Current head injury standards are based on accelerations and tests done with surface impacts to the forehead and cannot deduce what happens to the tissue inside the head [3]. Studies have often focused on either experimental or finite element brain injury prediction, but it will be useful to have both perspectives so that a broader understanding of what contributes to brain injury can be formed and experimental data can be validated. For a proper assessment of brain injury outcomes, this study will attempt to relate the mechanical input from an impact to the pressures developed within fluid that fills a human-like head model. This correlation will be validated using finite element method (FEM) simulation and the results from both of these sources will be compared to an analytical model for the pressures developed inside a fluid-filled shell. This work in particular will focus on the experimental setup and results for capturing the pressure and accelerations present on the head model during an impact.

Coup-contrecoup injuries are a group of focal brain injuries characterized by localized damage near the site of a head impact and directly opposite of the impact side. It has been observed frequently that brain injury to the site opposite to where an impact occurs can be more severe than injury to the area where the impact occurred [4]. It is best to measure the pressures developed inside a head during impact at the coup and contrecoup regions as that is where injurious phenomena are expected to take place. Figure 1 shows the expected pressure gradient at the site of impact and the opposite side.

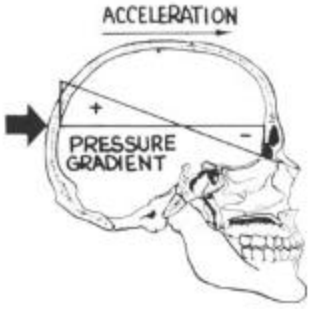

Figure 1. Representation of the Pressure Gradient Developed Inside a Head During Impact[5]

A study by Goeller in 2012 [6] used a shock tube to subject a fluid-filled human-like head model to a shockwave. In the study, cavitation was examined as a possible brain injury mechanism in the contrecoup region, and the pressures developed in a soft hydrogel material were measured in a similar manner to this study. The Goeller study is one of the very few studies to use both a finite element simulation and an experiment to examine the development of coup contrecoup pressures developed due to loading. Similarly, this study will examine the development of coup and contrecoup pressures due to loading, but in this case, the loading will be an impact from a pendulum arm rather than a shockwave passing over the head model.

Chapter 2
Experimental Methods and Setup

This work is in collaboration with other researchers. Figure 2 shows the multidisciplinary analysis conducted by the group members. Major collaboration has taken place between Mr. Aaron Jackson and myself (Mr. Arthur Koster). This study is broken up into two major parts, computational modeling, and the physical experiment. The experimental portion of this study is broken down into three categories consisting of the sensors, test platform, and head model. The contribution of this study to the experimental setup includes the selection of the data acquisition hardware and programming of the data acquisition software as well as the creation and testing of gelatin as a material to fill the head surrogate. This study also contributes the entirety of its experimental results to the overall research effort. The neck model that is connected to the head surrogate was created and the velocity of the pendulum at impact was verified by tracking the motion of the pendulum with a high-speed camera from Photron.

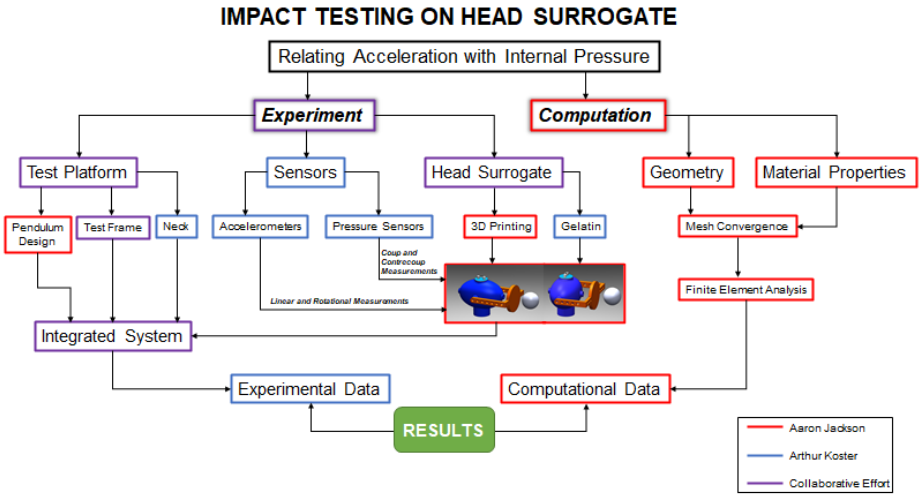

Figure 2. Breakdown of the Overall Research Effort Into Individual and Collaborative Tasks[7]

This study requires the measurement of the internal pressure and bulk acceleration during an impact to a head-like surrogate simultaneously. To accomplish this, pressure sensors, accelerometers, and a National Instruments Data Acquisition system (DAQ) were selected. Since an impact is a highly dynamic event, sufficient temporal resolution was necessary to ensure that the details of the impact event were resolved. Additionally, the sensing components needed to be able to withstand accelerations exceeding 500g. To power the sensors and Operational Amplifiers (OpAmps) used in the experiment, a DC power source was used. The pressure sensors and the OpAmps were

connected in parallel to a 10V DC source from the power supply. The accelerometers were connected in parallel to a 5V DC source provided by the DAQ. The pendulum was released by an electromagnet connected to a function generator that was set up as a DC power source. The electromagnet was powered by 10V.

1. Test Stand, Head Model, and Neck Model

An experimental setup was created based on the need to measure the internal pressure and bulk acceleration of a human head model subject to an external impact. A pendulum test stand was manufactured for the experiment out of hollow steel square stock welded into a frame. This frame was fixed to a base made from wood and concrete that helped to keep the frame rigid during an impact test. The baseplate was made from steel and also fixed to the wooden and concrete base. The baseplate had a slot so that the impact plate of the head model could be positioned at the bottom of the pendulum swing. The pendulum arm was made from hollow steel square stock and could be raised or lowered using an electromagnet attached to a winch. Figure 3 shows a diagram of the pendulum impactor. A digital angle measurement device was attached to the pendulum with magnets and the winch was used to raise the pendulum to the desired angle. Once the pendulum reached the desired angle, power to the electromagnet was turned off, the data acquisition started, and the impact commenced.

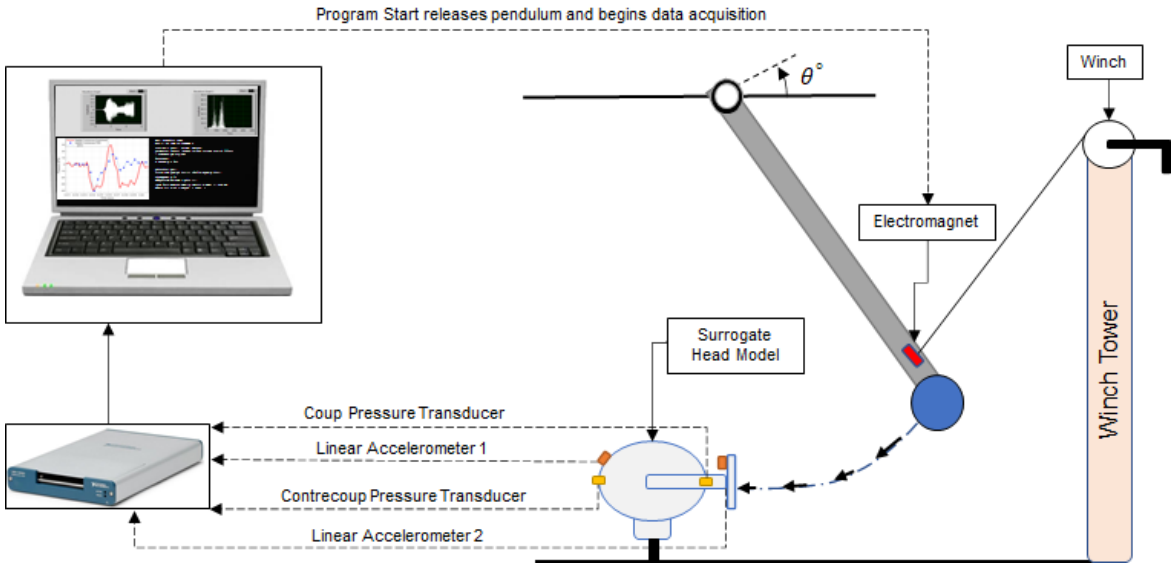

Figure 3. Diagram of the Pendulum Impactor and Head Model Setup [7]

A head model with a volume similar to that of an average adult and an elliptical cross-section was filled with water and gelatin to simulate a human head. The human head is a complex structure as it is made from several layers

of different materials that not only behave as engineering materials but also have electrical and biological properties. Although the head model used in this experiment is simplified, it provides useful information about the pressures developed inside the human head during an impact event. The portion of the head that is near the impact is called the coup and the portion of the head that is on the opposing side from the impact is called the contrecoup. Head models that simulated impacts and measured coup and contrecoup pressure responses were 3D printed for impacts normal to the coronal plane and the sagittal plane. An impact normal to the coronal plane simulates a frontal impact to the head while an impact normal to the sagittal plane simulates a side impact. The head models had an internal fluid volume of about 1212 ml which is slightly smaller than the average human head volume but still within an acceptable range [8]. Figure 4 shows a diagram of the head models used in the experiment as well as the coordinate system used by the accelerometers. Since different fluids with different mechanical properties can be tested inside the head model, the effects of an impact could be examined for various parts of the human head. Models were 3D printed from Nylon PA 12 on an HP powder-bed fusion printer.

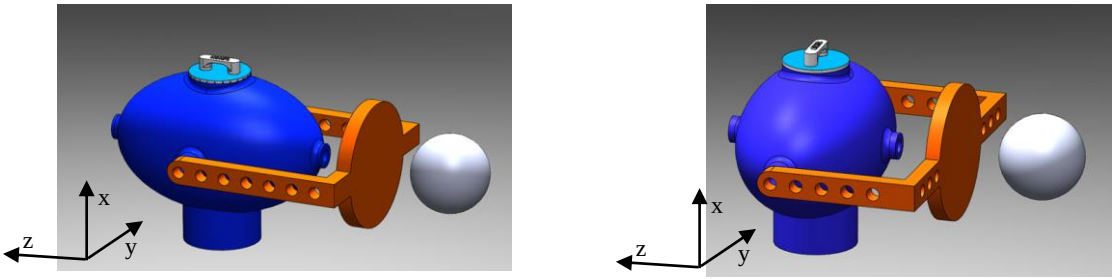

(a) **(b)**

Figure 4. (a) Head Model for Coronal Impact Plane (b) Head Model for Sagittal Impact Plane [7]

The neck model used in this experiment consisted of a pinewood dowel fixed inside of two 3D printed ABS ends that were connected to the head model and the baseplate. The baseplate was fixed to the wood and concrete base in a similar fashion to the pendulum test stand so that it would not move during an impact. Although a neck model with more bio-fidelity will be useful in future work related to impact testing on human head models, the current finite element simulation utilizes a fixed boundary condition. Therefore, to verify the experimental information with the finite element analysis, it is useful to fix the neck as much as possible during the impact. Once the finite element simulation, theory, and experiment can be compared accurately for a fixed boundary condition, the next step will be to use a neck model that shares more similarities with a human neck. The baseplate had a slot that allowed the impact plate to be positioned in exactly the correct position so that the pendulum was as close to traveling only in the horizontal direction as possible during the impact.

A theoretical prediction of the speed of the pendulum upon impact was performed using rigid body dynamics so that the speed of the pendulum could be used as a boundary condition in the FEM simulation. To verify this prediction, the speed of the pendulum just before impact could be calculated from frames captured by a high-speed camera. The high-speed camera was aligned perpendicular to the impact direction so that it could capture the impact with little to no error due to parallax. In the images from the high-speed camera, the dimensions of each pixel can be determined by measuring a known distance on the head model in terms of pixels. Using this scale and the position of the boundary between the dark background of the image and the illuminated pendulum impactor in each frame, the velocity of the impactor can be calculated. Figure 5 shows the theoretical pendulum velocity at impact and the velocity calculated using digital image correlation (DIC). Figure 6 shows three frames out of a video of an 80° pendulum release angle test.

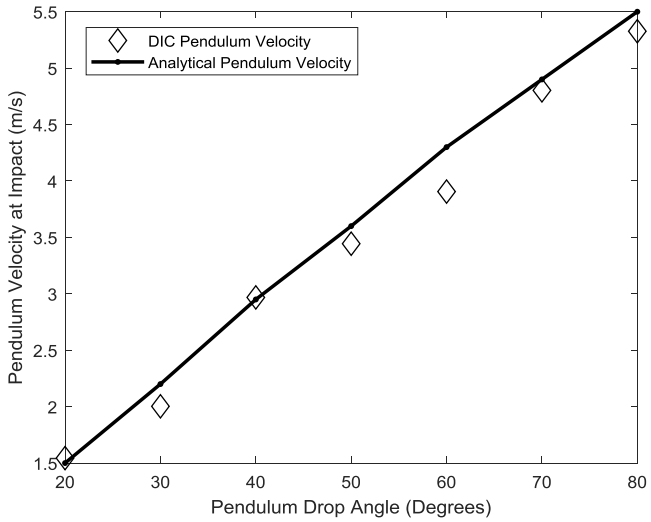

Figure 5. Analytical and Experimentally Calculated Pendulum Velocities at Impact with Pendulum Drop Angle

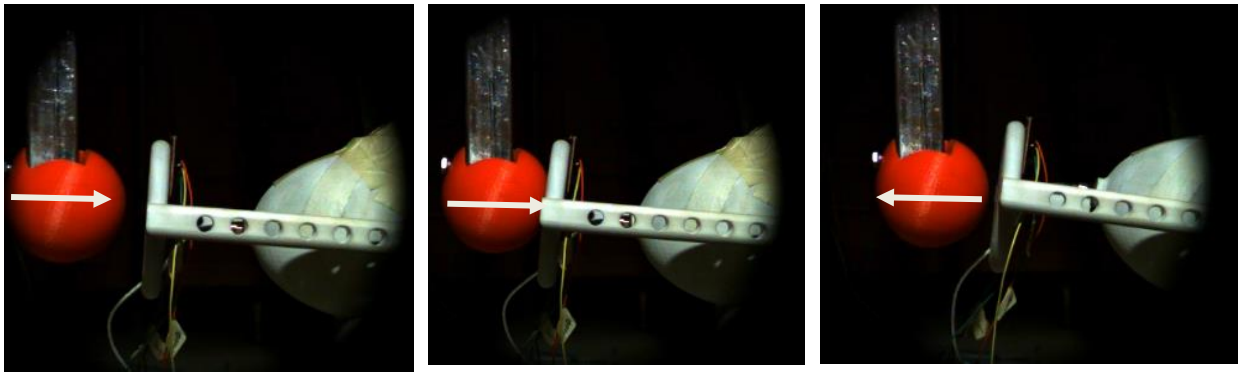

(a) **(b)** **(c)**

Figure 6. Images of the Pendulum and Head Model (a) Before, (b) During, and (c) After Impact

2. Sensor Selection

The pressure sensors selected for the experiment needed to be rugged, able to withstand an impact with a linear acceleration of 500g or greater with a large enough pressure range that if cavitation were to occur, there would not be any damage sustained to the sensor. Based on these requirements, the Kulite XTL-190-250SG was selected. This sensor can sustain accelerations of up to 10,000 g and can measure pressures up to 500 PSI which should be able to capture the collapse of a cavitation bubble should that occur during an impact test. This sensor is a differential voltage output, meaning that the measurement from the sensor comes from the data acquisition device measuring the difference in voltage between two leads from the sensor.

The accelerometer selected for the tests was the Mouser 832M1-0500 500g tri-axial accelerometer. This sensor was selected due to the versatility afforded by using a triaxial accelerometer and for its 500g acceleration sensing capacity. By using two of these accelerometers at different distances from the center of rotation, the rotational acceleration on the head model due to an impact can be calculated alongside the linear acceleration [9]. A diagram of the position of the accelerometers on the head model is shown in Figure 7.

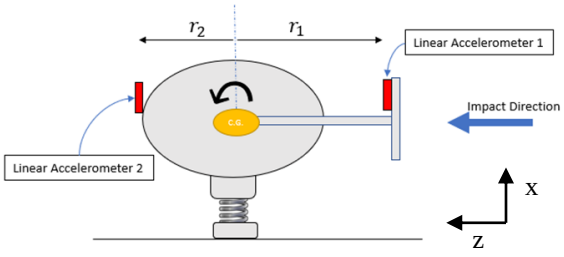

Figure 7. Head Model Diagram Showing the Accelerometer Locations for Measuring Rotational Acceleration [7]

$$Angular\ Acceleration = \frac{a_{x_1} - a_{x_2}}{r_1 - r_2} \quad (1)$$

Equation 1 shows the equation for calculating the angular acceleration of the head model where a_{x1} and a_{x2} are the accelerations from accelerometers one and two respectively and r_1 and r_2 are their distance to the center of rotation.

This sensor uses a referenced single-ended voltage output which means that the data acquisition device compares the voltage on the output lead of the sensor to electrical ground. The locations of the sensors on the head model are shown in Figure 8.

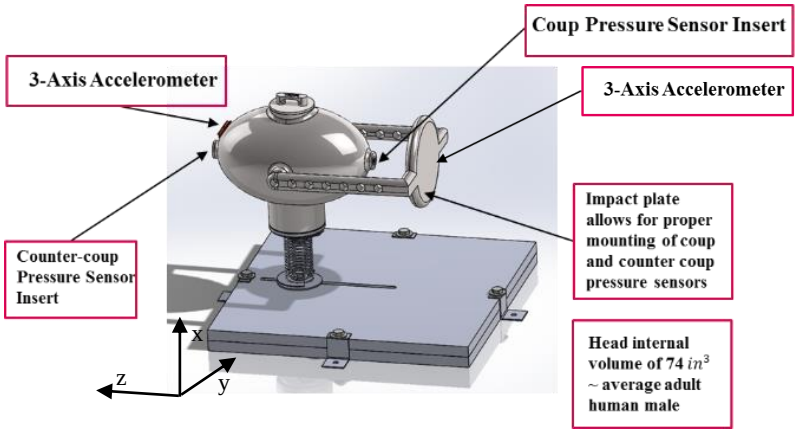

Figure 8. 3D Printed Human Head Surrogate with Sensor Locations and Base Plate

3. Data Acquisition

The output impedance of the pressure sensors was much greater than the input impedance of the NI DAQ which necessitated the implementation of a voltage follower circuit. A voltage follower circuit uses Operational Amplifiers (OpAmps) to lower the impedance across the leads of a device. In this case, since data sampling was occurring at such a high rate, the impedance of the input signal and input device needed to be closely matched to avoid the buildup of charge on the leads of the input device. A simple diagram of a typical differential voltage output sensor is shown in Figure 9 (a). Figure 9 (b) shows the same circuit after a voltage follower is added. In the case of this experiment, V_s represents the output voltage of the pressure sensor, R_s is the output impedance of the sensor, R_d is the input impedance of the DAQ, and R_0 is the output impedance across the voltage follower.

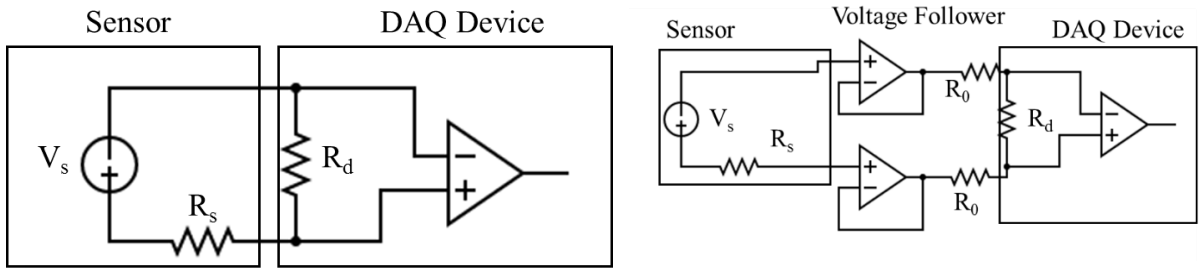

(a) **(b)**

Figure 9. (a) Circuit Diagram of a Typical Differential Voltage Output Sensor and DAQ Device (b) Circuit Diagram of a Typical Differential Voltage Output Sensor, Voltage Follower, and DAQ Device

$$Noise - Added(V_{rms}) = \sqrt{f(e_n^2 + (i_n R_s)^2)} \quad \textbf{2}$$

The operational amplifiers will add noise to the signal so it is useful to quantify this additional noise to determine how it will affect the experimental results. The noise introduced into the signal by the Op Amp can be determined using equation 2 where f is the bandwidth of the DAQ (3.4 MHz), e_n is the voltage noise density of the Op Amp (8 $nV/\sqrt{Hz}$), and i_n is the current noise density of the Op Amp ($pA/\sqrt{Hz}$). The source impedance, R_s, is 1 kΩ. The root mean square (RMS) noise generated by the Op Amps in the case of this experiment was 14.75 μV. This is three orders of magnitude less than the signal from the pressure sensor and corresponds to a pressure measurement of about 2.5 kPa and is an acceptable noise addition to the signal for the reduction in impedance.

The DAQ selected for this experiment needed to be able to capture a large amount of data sampled from analog devices in a highly dynamic environment while providing sufficient temporal resolution so that the pressure pulse and acceleration from the impact can be accurately studied. The DAQ selected was the National Instruments USB-6363. This system has the capability to capture one million samples per second across all channels combined. Since there were five total data channels from the sensors (two pressure sensors, one linear acceleration, and two rotational acceleration components) the maximum sampling rate possible was 200,000 samples per second per channel.

National Instruments LabVIEW software was used to capture and save the data from the measurement system. Inside the LabVIEW program, each sensor input was converted to either accelerations or pressure based on the sensitivity of each sensor. The signal from the pressure sensors possessed a noise profile of significant magnitude which necessitated the use of a low-pass filter. A study was conducted with a second-order digital Butterworth low-pass filter implemented in LabVIEW with varying cutoff frequencies to determine which best preserved the magnitude

of the pressure response while eliminating high-frequency noise. It was determined that using a frequency cutoff of 1000 Hz preserved much of the amplitude of the pressure response while greatly reducing the effects of noise on the signal. High-frequency events can still be captured by the system, but they are attenuated. The system captured two and a half seconds of data for every test for a total of 500,000 samples per data file. The data file output from LabVIEW was then acquired by a MATLAB program that plots the relevant data for visualization.

4. Gelatin Preparation

Gelatin concentrations of 0 g/ml (pure water), 0.05 g/ml, and 0.1 g/ml of water were used to simulate a range of mechanical properties meant to bound the range in which the properties of the human brain reside. The human brain is made mostly from grey and white matter but is contained within a head made from multiple layers of material comprised of skin, the skull, cerebrospinal fluid, arteries, and blood vessels. Since the brain resides in such a complex environment, it is necessary to perform impact tests with fluids that possess a variety of physical and mechanical properties. White matter has a Young's modulus of around 1.895 kPa while grey matter has a Young's modulus of around 1.389 kPa [10]. Gelatin solutions of 0 – 0.15 g/ml correspond to a range of Young's modulus of 0-110 kPa [11]]. The density of 0.05 g/mL gelatin solution is 1050 kg/m^3 while the density of human white matter and grey matter is 1040 kg/m^3 [3], [12]. The upper range of the Young's modulus for the gelatin concentrations tested in this experiment may exceed those of brain tissue, but the density is close to that of actual brain material.

To prepare a sample of gelatin, Type I DI water with a resistivity of about 18 MΩ-cm was mixed with Knox food-grade unflavored gelatin in concentrations of 0 g/ml, 0.05 g/ml, and 0.1 g/ml. The mixture was stirred constantly and heated to between 50°C and 60°C for a period of 30 minutes. The mixture was poured into the head surrogate models and cured for a period of about 16 hours at 4°C before being used in impact tests.

Chapter 3
Results and Discussion

Impact tests were conducted from pendulum release angles of 20° to 80° in 10° increments. The coronal and sagittal head models were impacted three times at each angle after being filled with water, 5% gelatin solution, and 10% gelatin solutions for a total of 63 impact tests. To relate the acceleration to the pressures developed inside the brain, linear acceleration could be used or rotational acceleration could be used. The pressure inside the material that fills the head or head model is a direct measurement that can reveal the degree of damage being done to the head. A head or head model subject to linear and rotational accelerations can have a wide, overlapping range of linear and rotational accelerations that produce injury and do not produce injury [3]. In a paper by Zhang et al.[3], linear accelerations that produced injury ranged from 32g to 102g while injurious accelerations ranged from 61g to 144g which is considerable overlap between injury and non-injury in terms of acceleration. Based on this, acceleration alone cannot reveal whether an injury occurs due to an impact to the head without being correlated to a direct measurement of the state of the material that, when damaged, produces a brain injury. Since the 1940s, many researchers of brain injury have believed that brain injury was caused either by linear or by rotational acceleration. While it may be true that head injury results from both of these phenomena, if the state of the material inside the head or head model can be measured and correlated with the rotational or linear acceleration and the phenomena that cause brain injury can be understood on multiple length scales, the threshold for head injury can be more accurately determined based on the direct measurement of the brain or head surrogate material. Rather than focus on the injury from accelerations, it would be more prudent to focus on the direct cause of brain injury which is the state of stress developed within the material of the brain during a damaging event which can be measured in part by measuring the hydrostatic pressure of the material [2]. A study by McLean in 1995 stated that there were not any cases of brain injury without the head experiencing a direct impact in over 400 studies of fatally injured road users [13]. Furthermore, purely linear acceleration produces a pressure gradient within the head while rotational acceleration produces shear stress [2]. Since rotational and linear accelerations are both indirect measurements of what happens inside the human head during an impact event, it will be useful to correlate the type of acceleration most closely associated with brain injury to the direct measurement of the internal material of the head model, a pressure measurement in this case. Based on this, the linear acceleration was correlated with the internal pressure of the fluid that filled the head model instead of the rotational acceleration.

1. Water Tests

Figure 10 and Figure 11 show the linear acceleration of the coronal and sagittal head models with the pendulum release angle. In the plots, each test is shown alongside the mean of three tests conducted at a single drop angle. The standard deviation is plotted using error bars.

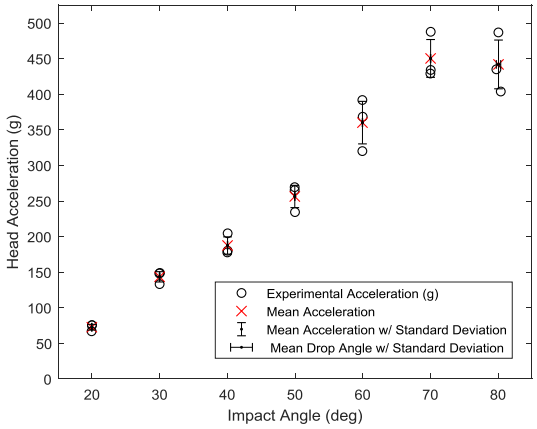

Figure 10. Bulk Coronal Head Surrogate Linear Acceleration with Pendulum Drop Angle

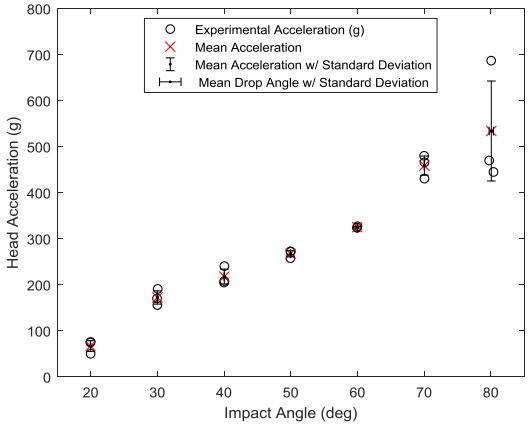

Figure 11. Bulk Sagittal Head Surrogate Linear Acceleration with Pendulum Drop Angle

These results are consistent with one another and show a nearly linear trend of acceleration with pendulum drop angle. Similarly, the results for the rotational acceleration can be seen in Figure 12 and Figure 13. These results also follow a mostly linear trend.

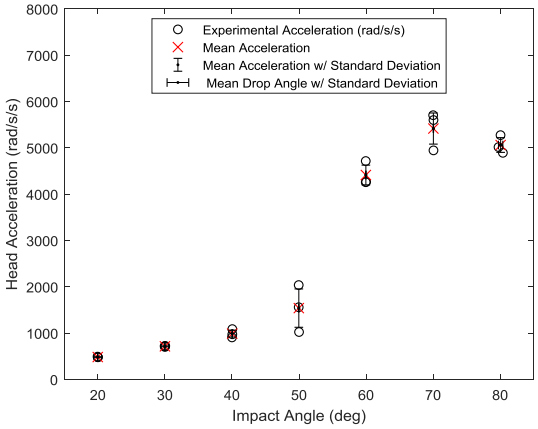

Figure 12. Bulk Coronal Rotational Acceleration with Pendulum Drop Angle

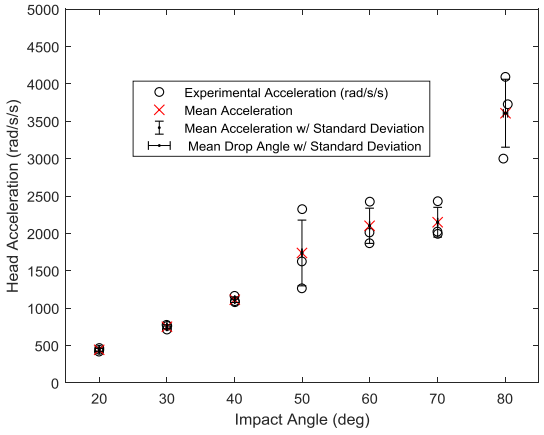

Figure 13. Bulk Sagittal Rotational Acceleration with Pendulum Drop Angle

The pressure spike above and below the ambient pressure measured by the pressure sensors is shown along with the linear acceleration of the head model during an impact test in Figure 14 and Figure 15. The legends of both

figures are included in Figure 15 for readability. In the sagittal plane, the maximum average linear acceleration produced by the pendulum impact on the head model was 381.7 ± 42.5g where g is gravity on earth (approximately 9.81 m/s^2). The maximum average rotational acceleration was 3608 ± 227 rad/s^2. The maximum average pressure spike in the coup region was 23.28 ± 0.38 kPa and the largest magnitude pressure spike in the contrecoup region was -37.36 ± 3.12 kPa. These results correspond to an 80° pendulum drop angle. In the Coronal plane, the maximum average linear acceleration was 450.3 ± 13.3g which occurred at a 70° drop angle. The maximum average rotational acceleration was 5063 ± 80 rad/s^2. The average pressure spikes of maximum magnitude were 96.94 ± 1.35 kPa and -47.29 ± 0.66 kPa for the coup and contrecoup respectively. The maximum rotational acceleration, as well as the maximum pressure spikes, occurred during the 80° impact tests whereas the maximum linear acceleration occurred during the 70° tests. This is likely due to the neck model, impactor, or test stand absorbing energy during impact during particularly energetic impacts. These results make physical sense as during the impact, the head model impinges on the fluid with which it is filled in the coup region while the head model moves "away" from the fluid near the contrecoup region creating a positive pressure spike in the coup region and a negative pressure spike in the contrecoup region. Additionally, the sagittal pressure response should be less than that of the coronal plane due to the reduced length along the axis of impact. To think of this simply using first-order analysis, the simple hydrostatic pressure due to the height of a fluid subject to acceleration is known to be $P_{hydrostatic}=\rho a l$ where ρ is the density of the fluid, a is the acceleration of the fluid, and l is the height of the fluid. In this case, and for a given acceleration and ρ, the pressure difference between the coronal and sagittal head models should be related to the length along the axis of the impact. $P_{hydrostatic}(coronal)-P_{hydrostatic}(sagittal)= \rho a(l_{coronal}-l_{sagittal})$. Since it is known that the coronal head model is longer than the sagittal, the pressure response should be of greater magnitude in the coronal plane and indeed that is what can be observed below. After performing a simple linear curve fit on these results, the relationship between the pressure spike and the linear acceleration of the head model is shown in Equations 3-6. These results show that for the coup region, a linear curve fit does not work quite as well as it does for the contrecoup region. This is possibly due to an increased sensitivity of the coup region to variations in the impact compared to the contrecoup region.

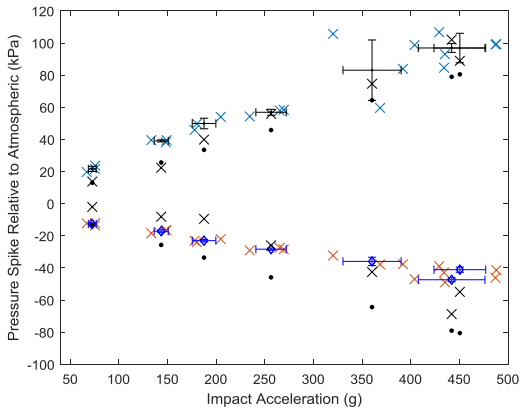

Figure 14. Coup and Contrecoup Pressure Spikes with Linear Impact Acceleration in the Coronal Plane

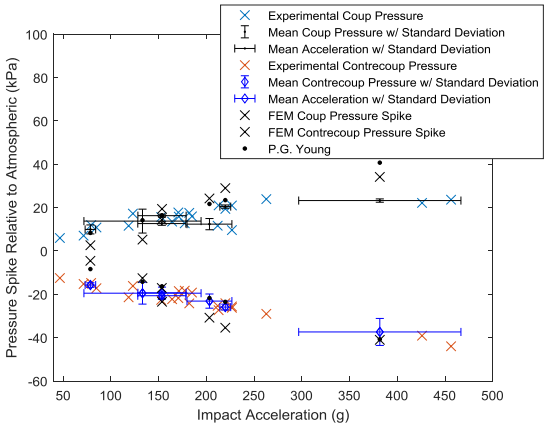

Figure 15. Coup and Contrecoup Pressure Spikes with Linear Impact Acceleration in the Sagittal Plane

$$\text{Coronal } \Delta P_{coup}=0.0277(A)+1.6419,\ R^2=0.8732 \quad \textbf{3}$$

$$\text{Coronal } \Delta P_{contrecoup}=-0.012(A)-0.966,\ R^2=0.9429 \quad \textbf{4}$$

$$\text{Sagittal } \Delta P_{coup}=0.0056(A)+1.2048,\ R^2=0.5599 \quad \textbf{5}$$

$$\text{Sagittal } \Delta P_{contrecoup}=-0.0105(A)-1.3645,\ R^2=0.9317 \quad \textbf{6}$$

These experimental tests show good agreement between the experiment, FEM simulation, and previous work done by P.G. Young to predict intracranial pressure due to an impact on a spherical, fluid-filled shell. Although this theory relies on the head model being spherical and the head model used in this experiment was elliptical, the results still closely align for coup region pressure spike. The P.G. Young model of intracranial pressure does not predict the pressure with time whereas the FEM simulation does. These results show that the initial pressure spike is similar in both the FEM and experimental data, but after the initial spike, differences can be observed. This is partially due to a difference between the damping that occurs in the experiment and the damping that occurs during the FEM simulation. The FEM simulation is necessarily a more simple model than the experiment, this is so that the relevant information can be captured without incurring a significant computational penalty. Another factor that will create a discrepancy between the simulation and experimental results is the difference in the neck model used in the experiment and the fixed boundary condition used in the FEM simulation. The fixed boundary condition sets the displacement of the base of the head model to zero throughout the entire impact while the head model moves due to mechanical backlash present in the neck during an experimental impact test. The initial pressure spike with time is similar between the FEM and the experiment and the average pressure spikes from the experiment are also closely aligned with the values of pressure predicted theoretically from the methods outlined in P.G. Young's work [14]. Figure 16 - Figure 19 shows the comparison between the experimental and FEM pressure with time plots [7].

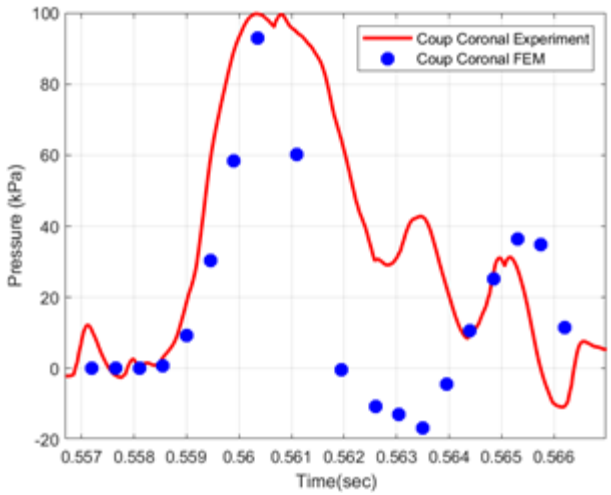

Figure 16. Comparison of Coronal Coup Pressure with Time Between Experimental and FEM Simulation Data [7]

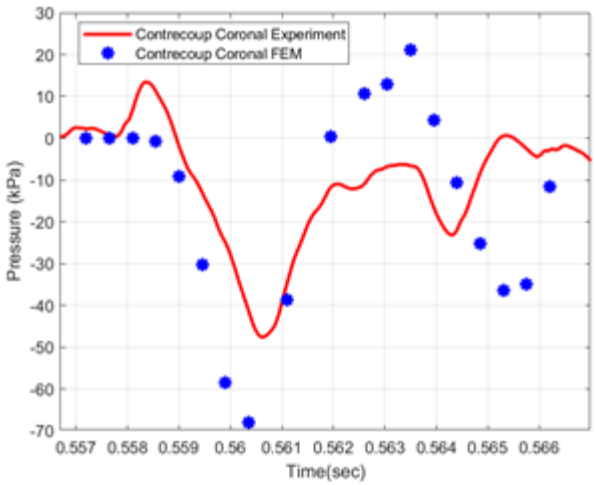

Figure 17. Comparison of Coronal Contrecoup Pressure with Time Between Experimental and FEM Simulation Data [7]

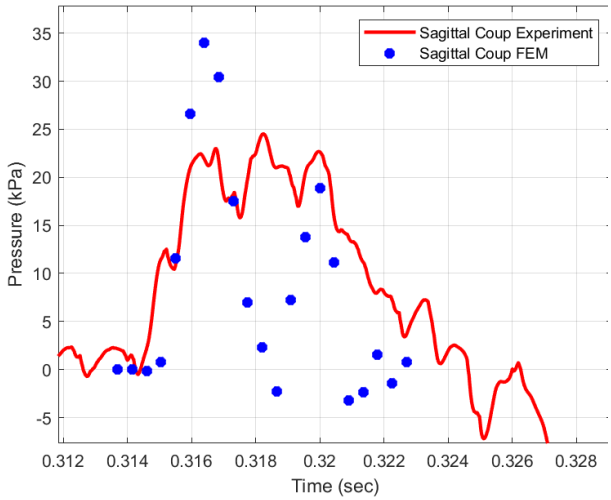

Figure 18. Comparison of Sagittal Coup Pressure with Time Between Experimental and FEM Simulation Data [7]

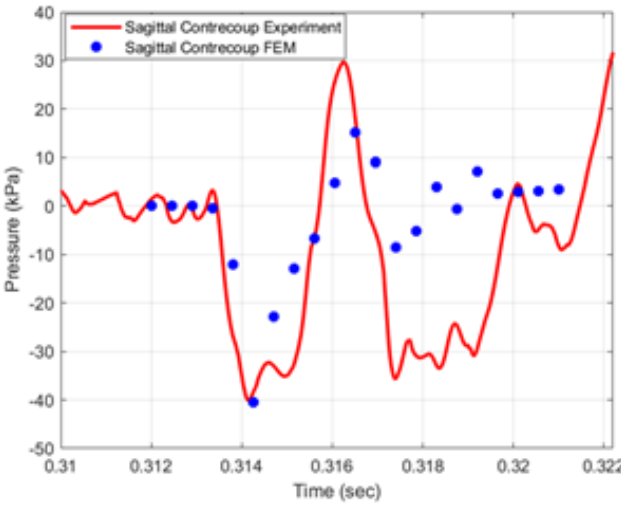

Figure 19. Comparison of Sagittal Contrecoup Pressure with Time Between Experimental and FEM Simulation Data [7]

2. Gelatin Tests

The pressure results for gelatin impact tests are expected to be of lower magnitude than the results for water because of the increased stiffness of gelatin compared to water [15]. The results are shown in Figure 20, Figure 21, Figure 22, and Figure 23. For 0.05 g/ml gelatin solution in the coronal plane, the maximum average pressure response was 44.97 ± 0.85 kPa and -30.5 ± .96 kPa for the coup and contrecoup respectively. This occurred at an average linear acceleration of 496 ± 25g, an average rotational acceleration of 3661 ± 247 rad/s^2, and a drop angle of 80°. In the sagittal plane, the maximum average pressure response was 23.66 ± 2.5 kPa for the coup region and occurred at a drop angle of 70°, a linear acceleration of 344 ± 4.9g, and rotational acceleration of 1694 ± 699 rad/s^2. In the contrecoup

region, the maximum mean pressure spike was -19.09 ± 1.72 kPa and occurred at a drop angle of 40°, a mean linear acceleration of 132 ± 2.75g, and a mean angular acceleration of 904.2 ± 13.2 rad/s^2. For the 0.1 g/ml gelatin solution in the coronal plane, the maximum average pressure response was 13.1 ± 0.7 kPa in the coup at 80° pendulum release angle which corresponds to a mean linear acceleration of 347 ± 27.5g and a mean rotational acceleration of 1632 ± 21.5 rad/s^2. In the contrecoup region the largest average pressure drop occurred at 80° alongside the maximum coup response with a pressure drop of -34.1 ± 5.7 kPa. In the sagittal plane, the maximum pressure response in the coup and contrecoup regions was 56.7 ± 5.05 kPa and -18.6 ± 0.63 kPa with the maximum coup response happening at a drop angle of 80° while the maximum contrecoup response happened at a drop angle of only 20°, although the pressure response of the contrecoup is close to this same value at the other pendulum drop angles tested. Equations represent a linear curve fit of the pressure versus linear acceleration data.

$$\text{0.05 g/ml Coronal } \Delta P_{coup}=0.0096(A)+1.9486,\ R^2=0.7665 \quad (7)$$

$$\text{0.05 g/ml Coronal } \Delta P_{contrecoup}=-0.0052(A)-2.3243,\ R^2=0.6208 \quad (8)$$

$$\text{0.05 g/ml Sagittal } \Delta P_{coup}=0.0037(A)+1.6667,\ R^2=0.3418 \quad (9)$$

$$\text{0.05 g/ml Sagittal } \Delta P_{contrecoup}=-0.0016(A)-1.7464,\ R^2=0.1673 \quad (10)$$

$$\text{0.1 g/ml Coronal } \Delta P_{coup}=0.0014(A)+1.3193,\ R^2=0.5576 \quad (11)$$

$$\text{0.1 g/ml Coronal } \Delta P_{contrecoup}=-0.0101(A)-1.0934,\ R^2=0.7693 \quad (12)$$

$$\text{0.1 g/ml Sagittal } \Delta P_{coup}=0.0116(A)+1.2502,\ R^2=0.7233 \quad (13)$$

$$\text{0.1 g/ml Sagittal } \Delta P_{contrecoup}=-0.0005(A)-2.1776,\ R^2=0.0199 \quad (14)$$

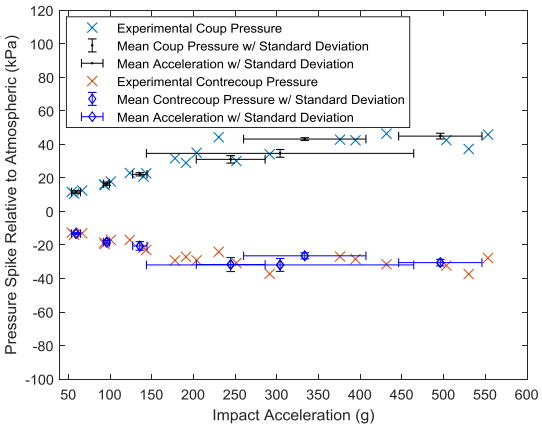

Figure 20. 0.05g/ml Gelatin Solution Coronal Coup and Contrecoup Pressure Spikes with Impact Acceleration

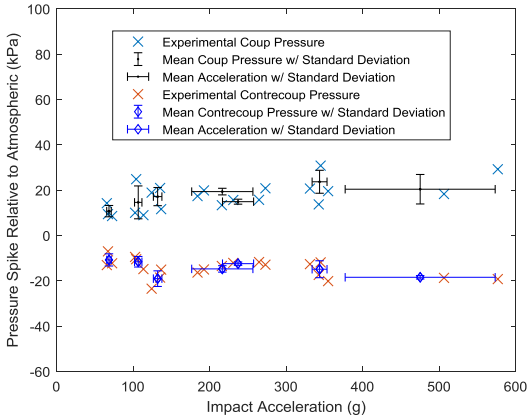

Figure 21. 0.05g/ml Gelatin Solution Sagittal Coup and Contrecoup Pressure Spikes with Impact Acceleration

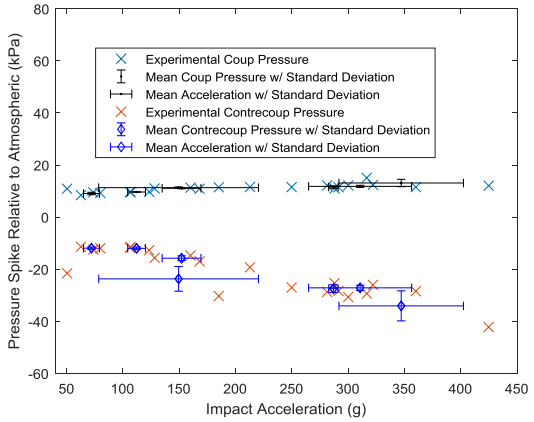

Figure 22. 0.1g/ml Gelatin Solution Coronal Coup and Contrecoup Pressure Spikes with Impact Acceleration

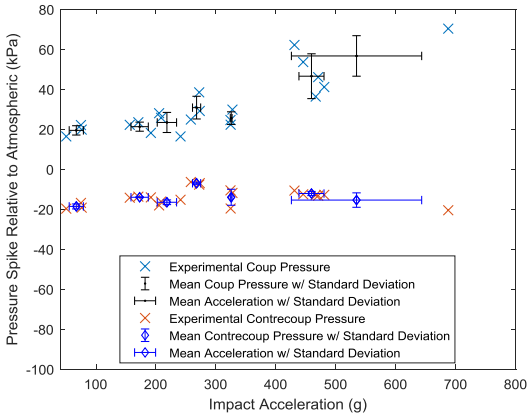

Figure 23. 0.1g/ml Gelatin Solution Sagittal Coup and Contrecoup Pressure Spikes with Impact Acceleration

Compared to the water tests, the gelatin tests were expected to produce pressure results of less magnitude than those observed in the water tests due to the increased Young's modulus of gelatin compared to water. This was true in most cases, however, for the case of the sagittal 0.1 g/ml tests, a higher magnitude pressure response was observed in the coup region of the head. This is in part due to the fact that the head model underwent a higher magnitude acceleration in the tests that produced the higher magnitude pressure responses. In the other cases of the gelatin tests, the observed pressure responses were less than those observed in the water tests, but they did not fit a linear trend like the water pressure spikes.

Using the velocity of the pendulum at impact from the rigid body dynamics analysis, the momentum of the pendulum at impact can be calculated. The time that it takes for this velocity to be imparted can be determined from experimental data. This is around 2 milliseconds for the impact tests conducted in this study. Assuming that the total

momentum of the pendulum is transferred to the head model and that it begins at rest, the theoretical change in velocity of the head model can be calculated. Using the theoretical change in velocity of the head model and the time it takes to impart this velocity, the acceleration can be calculated for each test. The impact is assumed to be only in the horizontal direction for simplicity. Using the experimental data for the water tests, the average energy dissipated into the neck model, pendulum arm, and test frame can be estimated. Table I shows the experimental acceleration alongside the acceleration estimated by the previous analysis.

Table I Experimental and Estimated Accelerations with Pendulum Release Angle

Pendulum Release Angle	Experimental Acceleration (g)	Calculated Acceleration (g)	Percent Difference
20°	72.72	132	57.9%
30°	143.51	193.6	30.1%
40°	187.53	259.6	32.3%
50°	256.39	316.9	21.1%
60°	360.14	378.5	4.97%
70°	450.32	431.3	4.31%
80°	441.91	484.2	9.13%

This analysis shows that energy is being dissipated by the experimental setup during impact tests instead of being transferred directly to the head model. More energy is being dissipated during the low impact angle tests than the high impact angle tests. It can be observed that energy is being dissipated in the flexible impact ball, the neck model, the pendulum itself, and the test frame. At the low impact angles, the pendulum rebounds more than at the high impact angles which could be why more energy is dissipated at these angles.

Another possible source of error in this experiment other than the energy dissipation is that the maximum pressure in the fluid may not occur at the position of the sensors in the head model. In the FEM simulation, the maximum pressure sustained to the inside of the head model was slightly below the position of the pressure sensors although the pressure spike reported was measured at the position of the sensors [7]. During different impact tests, slight differences between one impact and another such as the angle to which the impact plate was set relative to the head model could cause the position of the maximum pressure in the fluid to change.

Chapter 4
Conclusions

Brain injury is a main cause of traumatic injury in the United States and can be directly linked to internal brain material damage. Current head injury criteria are based on linear and rotational acceleration as well as skull fracture from forehead impacts. It was necessary to try to link the accelerations of a head model to pressures that develop within. In this study, research has been performed to understand the internal state of the pressure of the fluid that is inside a human-like head model subject to an impact event. Since brain injury is closely related to damaging pressures developed inside the head and the state of the fluid subject to an impact test can be linked to the mechanical excitation on the system, this study is able to more closely link the physical loading conditions of the bulk head model with the phenomenon that is a main source of brain injury. A unique pendulum impact test setup was created using pressure sensors, accelerometers, a NI DAQ, and NI LabVIEW software. Using two different gelatin solutions as well as water, fluids and soft materials with a range of mechanical properties could be tested inside the head model to simulate the range of mechanical properties found in biomaterials. This study found that for the coup region for a water-filled head model, the pressure responses during impact did correlate loosely to a linear trend with R^2 values of 0.8732 and 0.5599 for the coronal and sagittal planes respectively. For the contrecoup region, the pressure response was correlated more strongly with a linear trend with R^2 values of 0.9429 and 0.9317 for the coronal and sagittal planes respectively. Testing with gelatin revealed a lower magnitude pressure response than with water except in one case of the 0.5 g/ml sagittal coup response. The pressure spikes from the gelatin tests results do not correlate well with a linear trend, but the magnitude of the pressure spikes does slightly increase as the impact becomes more energetic.

Future work will take the idea of correlating the impact acceleration directly to the internal phenomenon of the head model one step further by placing live cell cultures in a head model that is a more biofidelic representation of a human head from True Phantom Solutions. Using a microscope, the cells will be imaged before and after impacts of differing severity to understand how the mechanical input to the head model relates to the health of the cells within a human brain.

References

[1] J. F. Kraus and D. L. McArthur, "EPIDEMIOLOGIC ASPECTS OF BRAIN INJURY," *Neurologic Clinics*, vol. 14, no. 2, pp. 435–450, May 1996, doi: 10.1016/S0733-8619(05)70266-8.

[2] A. King, K. Yang, and L. Zhang, "Is Head Injury Caused by Linear or Angular Acceleration? Injury predictors for traumatic axonal injury in a rodent head impact acceleration model View project Projects in impact biomechanics View project," 2003. [Online]. Available: https://www.researchgate.net/publication/242211067

[3] L. Zhang, K. H. Yang, and A. I. King, "A Proposed Injury Threshold for Mild Traumatic Brain Injury," *Journal of Biomechanical Engineering*, vol. 126, no. 2, pp. 226–236, Apr. 2004, doi: 10.1115/1.1691446.

[4] L. B. Drew and W. E. Drew, "New Perspectives in Brain Injury The Contrecoup-Coup Phenomenon A New Understanding of the Mechanism of Closed Head Injury," 2004.

[5] A. G. Gross, "A NEW THEORY ON THE DYNAMICS OF BRAIN CONCUSSION AND BRAIN INJURY*."

[6] J. Goeller, A. Wardlaw, D. Treichler, J. O'Bruba, and G. Weiss, "Investigation of cavitation as a possible damage mechanism in blast-induced traumatic brain injury," *Journal of Neurotrauma*, vol. 29, no. 10, pp. 1970–1981, Jul. 2012, doi: 10.1089/neu.2011.2224.

[7] A. Jackson, "INTERNAL PRESSURE RESPONSE OF A HUMAN HEAD SURROGATE MODEL SUBJECT TO VARIABLE IMPACT LOADING WITH FINITE ELEMENT VALIDATION ," Arlington, 2021.

[8] V. S. Caviness, D. N. Kennedy, C. Richelme, J. Rademacher, and P. A. Filipek, "The Human Brain Age 7-11 Years: A Volumetric Analysis Based on Magnetic Resonance Images." [Online]. Available: https://academic.oup.com/cercor/article/6/5/726/497980

[9] "Using Two Tri-Axis Accelerometers for Rotational Measurements," 2015. [Online]. Available: www.kionix.com

[10] S. Budday *et al.*, "Mechanical properties of gray and white matter brain tissue by indentation," *Journal of the Mechanical Behavior of Biomedical Materials*, vol. 46, pp. 318–330, Jun. 2015, doi: 10.1016/j.jmbbm.2015.02.024.

[11] A. Markidou, W. Y. Shih, and W. H. Shih, "Soft-materials elastic and shear moduli measurement using piezoelectric cantilevers," *Review of Scientific Instruments*, vol. 76, no. 6, 2005, doi: 10.1063/1.1928407.

[12] F. Hasan, K. A. H. al Mahmud, M. I. Khan, S. Patil, B. H. Dennis, and A. Adnan, "Cavitation Induced Damage in Soft Biomaterials," *Multiscale Science and Engineering*, vol. 3, no. 1, pp. 67–87, Mar. 2021, doi: 10.1007/s42493-021-00060-x.

[13] A. J. McLEAN, "Brain Injury without Head Impact?," *Journal of Neurotrauma*, vol. 12, no. 4, pp. 621–625, Aug. 1995, doi: 10.1089/neu.1995.12.621.

[14] P. G. Young, "An analytical model to predict the response of fluid-filled shells to impact - A model for blunt head impacts," *Journal of Sound and Vibration*, vol. 267, no. 5, pp. 1107–1126, Nov. 2003, doi: 10.1016/S0022-460X(03)00200-1.

[15] W. Kang, A. Ashfaq, T. O'shaughnessy, and A. Bagchi, "Cavitation Nucleation in Gelatin: Experiment and Mechanism," 2017.